https://doi.org/10.5194/bg-2023-137
Preprint. Discussion started: 28 August 2023

Biogeosciences Discussions
Open Access
EGU

Evaluation of five models for constructing forest NPP-age relationships in China based on 3121 field survey samples

Peng Li[1,2], Rong Shang[1,2*], Jing M. Chen[1,3*], Mingzhu Xu[1,2], Xudong Lin[1,2], Guirui Yu[4], Nianpeng He[4], Li Xu[4]

[1] Key Laboratory for Humid Subtropical Eco-Geographical Processes of the Ministry of Education, School of Geographical Sciences, Fujian Normal University, Fuzhou, 350007, China
[2] Academy of Carbon Neutrality, Fujian Normal University, Fuzhou 350007, China
[3] Department of Geography and Planning, University of Toronto, Ontario, ON M5S 3G3, Canada
[4] Key Laboratory of Ecosystem Network Observation and Modeling, Institute of Geographic Sciences and Resources Research, Chinese Academy of Sciences, Beijing, 100101, China

Correspondence to: Rong Shang (shangrong@fjnu.edu.cn) and Jing M. Chen (jing.chen@utoronto.ca)

https://doi.org/10.5194/bg-2023-137
Preprint. Discussion started: 28 August 2023

Biogeosciences Discussions

Abstract. Forest net primary productivity (NPP), representing the biomass carbon gain from the atmosphere, varies significantly with forest age. Reliable forest NPP-age relationships are essential for forest carbon cycle modelling and prediction. These relationships can be derived from forest inventory or field survey data, but it is unclear which model is the most effective for simulating forest NPP variation with age. Here, we aim to establish NPP-age relationships for China's forests based on 3121 field survey samples. Five models, including the Semi-Empirical Mathematical (SEM) function, the Second-Degree Polynomial (SDP) function, the Logarithmic (L) function, the Michaelis-Menten (M) function, and the Γ function, were compared against field data. Results of the comparison showed that the SEM and the Γ function performed much better than the other three models. SEM also outperformed the Γ function in tracking forest NPP-age curves at old ages and therefore is regarded as the best NPP-age model. The finalized forest NPP-age curves for five forest types in six regions of China can facilitate forest carbon modelling and future carbon projections in China and may also be useful for other regions.

1 Introduction

Forests play a critical role in sequestering atmospheric carbon dioxide (Hicke et al., 2007; Liu et al., 2012; Eggleston et al., 2006; Pan et al., 2011) and mitigating climate change (Friedlingstein, 2020). Forest net primary productivity (NPP), which represents the biomass carbon gain from the atmosphere (Fang et al., 2001; Chapin et al., 2006), constitutes the largest component of the terrestrial carbon cycle (Alexandrov et al., 1999; Hasenauer et al., 2004; Zha et al., 2013; Zhao and Zhou, 2005). It varies significantly with forest age (Bond-Lamberty et al., 2004; Wang et al., 2007, 2011), featured by an initial increase at young ages, a maximum at a middle age, and then a gradual decline at old ages (Yu et al., 2017; He et al., 2012). Building forest NPP-age curves is therefore essential in forest carbon modelling (Luyssaert et al., 2008).

Forest NPP-age curves differ considerably for different regions and forest types due to their unique compositions and diverse growth environments (Yu et al., 2017; He et al., 2012). In Europe (Zaehle et al., 2006), Canada (Chen et al., 2003), and America (Guo et al., 1955; He et al., 2012), forest NPP-age curves have been established for different forest types or regions. However, these curves can't be directly used for China's forest carbon modelling. To address this issue, some studies have tried to build forest NPP-age curves in China. Yu et al. (2017) established forest NPP-age curves for twelve major forest types in Heilongjiang province using forest inventory data and yield tables. Wang et al. (2018) derived forest NPP-age curves for nine pure forest types with different site indices within Heilongjiang province using the yield tables, biomass equations, and forest inventory data. Zheng et al. (2019) built two forest NPP-age curves separately for coniferous and broad-leaved forests in Zhejiang province using forest inventory data. But these curves are limited to the provincial level (currently only available in Heilongjiang and Zhejiang provinces), and cannot represent the diverse growth status of China's forests. Wang et al. (2011) constructed five forest NPP-age curves for five representative forest ecosystems in China, but the NPP data used to build these curves were obtained from the simulations of the BEPS (Boreal Ecosystem Productivity Simulator) model (Chen et al., 2012; Ju et al., 2006; Liu et al., 2002, 1999), not forest inventory data or field survey data. Furthermore, these curves didn't consider the significant differences in forest and climate conditions between the north and south of China and were insufficient to

https://doi.org/10.5194/bg-2023-137
Preprint. Discussion started: 28 August 2023

differentiate the north-south variations in China (Dai et al., 2011). Therefore, it is essential to develop forest NPP-age curves for the entire China with consideration of the differences in regions and forest types.

There were some models that could be used to simulate the forest NPP-age curves (Chen et al., 2003; Yu et al., 2017; He et al., 2012; Peper et al., 2001; Semenzato et al., 2011; Dalgleish et al., 2015; Tang et al., 2014). The Semi-Empirical Mathematical (SEM) function was first developed for simulating NPP-age relationships in Canada (Chen et al., 2003), America (He et al., 2012), and China (Wang et al., 2011; Yu et al., 2017; Wang et al., 2018; Zheng et al., 2019). The Second-Degree Polynomial (SDP) function, Logarithmic (L) function, Michaelis-Menten (M) function, and Γ function were used to build the NPP-age relationships for the boreal and temporal forests (Tang et al., 2014). The L function was mainly used to construct the relationship between diameter at breast height (DBH), forest height, and forest age (Peper et al., 2001; Semenzato et al., 2011; Dalgleish et al., 2015), and it was also used to model NPP-age relationships (Tang et al., 2014) as forest NPP is related with DBH and forest height. The M function is a common mathematical model used to describe enzyme reaction kinetics (Do et al., 2022), and was also found to be suitable for relating carbon fluxes to forest age (Tang et al., 2014). The Γ function was demonstrated to have better performance than the SDP function, L function, and M function in building the NPP-age relationships for the boreal and temporal forests (Tang et al., 2014). Different models could show diverse performance in tracking forest NPP-age curves for different forest types and regions. To facilitate the forest carbon modelling, it is crucial to compare these models in building forest NPP-age curves across diverse forest types and regions in China.

There are two objectives of this study: (1) to build forest NPP-age relationships for the entire China considering differences in regions and forest types based on forest field survey data and remote sensing data, and (2) to compare five models and determine the optimal model in building forest NPP-age relationships across China. As 33%−50% of forest NPP is allocated to foliage and fine roots each year (Gower et al., 1997), the forest field NPP was calculated from forest field survey data considering three components (Chen et al., 2002; He et al., 2012): total biomass increase (sum of the stem, branch, and coarse root biomass), turnovers of foliage, and turnovers of fine roots in the soil. To capture the diverse NPP-age relationships across different regions and forest types in China, we classified the country into six regions and five representative forest types.

2 Study Area and Data

2.1 Study area

China is selected as the study area, and its forests include five cover types: Evergreen Broad-leaved Forests (EBF), Evergreen Needle-leaved Forests (ENF), Deciduous Broad-leaved Forests (DBF), Deciduous Needle-leaved Forests (DNF), and Mixed Forests (MF). According to China's geographical division (Fang et al., 2001), the study area was divided into six regions (Fig. 1): Northeast China (NE), North China (N), Northwest China (NW), East China (E), Southwest China (SW), and South China (S). Significant differences in forest cover types can be observed among different regions. Region NE (including Heilongjiang, Jilin, and Liaoning provinces) is a typical boreal forest in the world and the most significant natural forest area in China. Region N (including Beijing and Tianjin cities, and Hebei, Shanxi, and Inner Mongolia provinces) accounts for 14% of China's

https://doi.org/10.5194/bg-2023-137
Preprint. Discussion started: 28 August 2023

total forest area and is mainly composed of DBF and ENF. Regions NW (including Gansu, Ningxia, Qinghai, Shanxi, and Xinjiang provinces) only account for 2.57% of the total forest area in China. Region E (including Shanghai City and Jiangsu, Zhejiang, Anhui, Fujian, Jiangxi, Shandong, and Taiwan provinces) accounts for 14% of China's total forest area, and its forests show significant zonal characteristics. Region SW (including Yunnan, Sichuan, Xizang, Guizhou, and Chongqing provinces) is the second-largest natural forest area in China, accounting for 26% of China's total forest area and 43% of China's forest stock (Liu et al., 2021). Region S (including Henan, Hubei, Hunan, Guangdong, Guangxi, and Hainan provinces) accounts for 20% of the total forest area in China with a large proportion of planted forests.

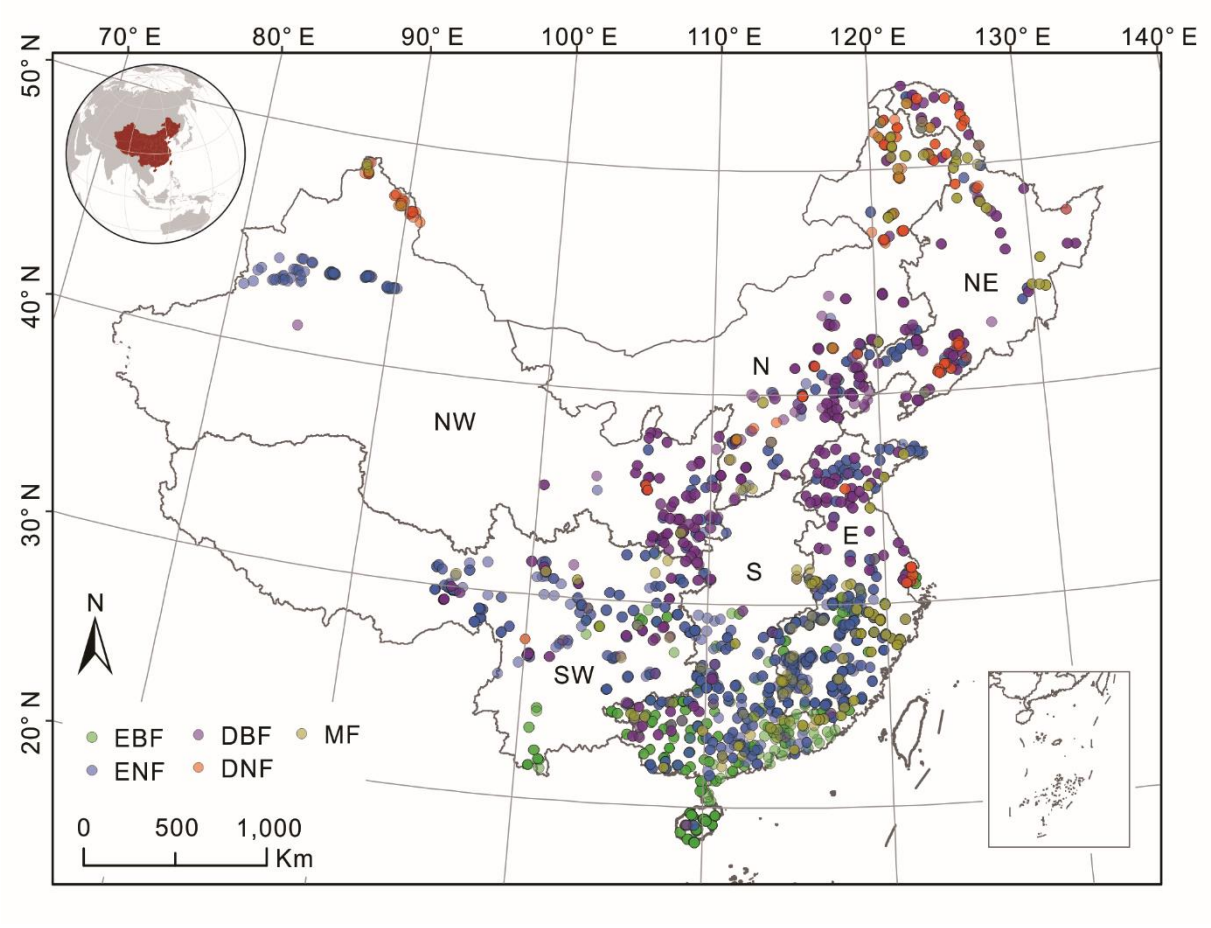

Figure 1. Distribution of forest field survey sites and their forest cover types (different colour indicates different types) within the six regions of China. E: Northeast China; N: North China; NW: Northwest China; E: East China; S: South China; SW: Southwest China; EBF: Evergreen Broad-leaved Forests; ENF: Evergreen Needle-leaved Forests; DBF: Deciduous Broad-leaved Forests; DNF: Deciduous Needle-leaved Forests; MF: Mixed Forests.

2.2 Data

The forest field survey data (Fang et al., 2018) and the GLOBMAP Version 3 LAI product (Liu et al., 2012) were used to build forest NPP-age curves for different regions and forest types.

https://doi.org/10.5194/bg-2023-137
Preprint. Discussion started: 28 August 2023

The forest field survey data includes 3121 sampling sites across China (Figure 1) except for Taiwan, Hongkong, and Macao (Fang et al., 2018). It includes 585 EBF sites, 1340 ENF sites, 745 DBF sites, 196 DNF sites, and 255 MF sites. These sites were selected according to their representativeness of the forest types in a given area, and they were sampled using the method outlined by the Intergovernmental Panel on Climate Change (IPCC) (Tang et al., 2018). This dataset records the site location, survey time, forest cover type, stand age, forest aboveground biomass, forest underground biomass, and so on. These attributes were first used to calculate the forest field NPP and then build the forest NPP-age curves.

The GLOBMAP Version 3 LAI product (Liu et al., 2012) was mainly used in the calculation of forest foliage biomass as part of NPP. It provides consistent long-term global leaf area index (LAI) data at 500 m spatial resolution from 1981 to 2022 on a geographical grid by fusion of Moderate Resolution Imaging Spectroradiometer (MODIS) and Advanced Very High-Resolution Radiometer (AVHRR) data. According to the site location and survey time, the matched LAIs were used to calculate the turnovers of foliage and turnovers of fine roots in the soil.

3 Methods

3.1 Calculating forest field NPP

Forest field NPP was not directly provided by the forest field survey data, and it was calculated from four components (Chen et al., 2002; Xia et al., 2019):

$$NPP = \triangle B_c + M + L_l + L_{fr}, \quad (1)$$

where $\triangle B_c$ is the annual increment of total living biomass including stems, branches, and coarse roots; M is the mortality per year that includes standing dead trees and fallen dead trees; L_l is the turnover of leaves per year; and L_{fr} is the turnover of fine roots per year in the soil. Mortality (M) is ignored in this study due to a lack of observations at the ground plots and its small proportion of NPP (3.7% of NPP on average using the observations from the USA (He et al., 2012)).

The annual increment of total living biomass was calculated from the annual biomass change ($\triangle B$) and the ratio from biomass to carbon (c) (White et al., 2000; Xia et al., 2019). The c was set to 0.5 following previous studies (Van Tuyl et al., 2005; Fang et al., 2001; Pan et al., 2011).

$$\triangle B_c = \triangle B \times c, \quad (2)$$

The calculation of the leaf renewal rate (L_l) is related to leaf area index (LAI), specific leaf area (SLA), leaf turnover rate (t_l), and carbon content (c):

$$L_l = \frac{LAI}{SLA} \times t_l \times c, \quad (3)$$

The amount of fine root regeneration is closely related to the amount of leaf regeneration, and hence the proportions of NPP allocated to fine root and leaf are related:

https://doi.org/10.5194/bg-2023-137
Preprint. Discussion started: 28 August 2023

$$L_{fr} = R_{fr,l} \times L_l, \quad (4)$$

where, $R_{fr,l}$ represents the ratio of carbon allocated to new fine roots to carbon in new leaves. Table 1 provides detailed values for the coefficients of SLA, t_l, and $R_{fr,l}$ for different forest types (White et al., 2000). The coefficients of MF were calculated as the average value of the other four forest cover types.

Table 1. The input parameters in the calculation of NPP for different forest types. SLA is the specific leaf area; $\boldsymbol{t_l}$ is the foliage turnover ratio; $\boldsymbol{R_{fr,l}}$ is the ratio of NPP to fine roots and leaves. EBF: Evergreen Broad-leaved Forests; ENF: Evergreen Needle-leaved Forests; DBF: Deciduous Broad-leaved Forests; DNF: Deciduous Needle-leaved Forests; MF: Mixed Forests.

Forest Type	SLA (m^2 kg C^{-1})	t_l ($year^{-1}$)	$R_{fr,l}$ (kg C kg C^{-1})
EBF	32.000	1.000	1.200
ENF	8.200	0.260	1.400
DBF	32.000	1.000	1.200
DNF	22.000	1.000	1.200
MF	23.550	0.815	1.300

3.2 Building forest NPP-age relationships

Five models, including the SEM function, SDP function, L function, M function, and Γ function, were used to build the NPP-age relationships among the five forest cover types and six regions in China.

The SEM function (Chen et al., 2003; He et al., 2012) is as follows:

$$NPP(i) = a\left[1 + (b(i/c)^d - 1)/e^{(i/c)}\right], \quad (5)$$

where *a*, *b*, *c*, and *d* are empirical coefficients to be determined from data, and $NPP(i)$ is NPP at the age of i.

The SDP function (Tang et al., 2014) is as follows:

$$NPP(i) = a \times i^2 + b \times i + \mathrm{c}, \quad (6)$$

where *a*, *b*, and *c* are empirical coefficients.

The L function (Peper et al., 2001; Semenzato et al., 2011; Dalgleish et al., 2015) is as follows:

$$NPP(i) = a[\log(i+1)]^b, \quad (7)$$

where *a* and *b* are empirical coefficients.

The M function (Tang et al., 2014; Do et al., 2022) is as follows:

$$NPP(i) = a \times i/(b+i), \quad (8)$$

where *a* and *b* are empirical coefficients.

The Γ function (Tang et al., 2014) is as follows:

$$NPP(i) = k_0 i^{k_1} e^{k_2 \cdot i}, \quad (9)$$

https://doi.org/10.5194/bg-2023-137
Preprint. Discussion started: 28 August 2023

where k_0, k_1, and k_2 are empirical coefficients.

The R^2 and RMSE were used to determine the optimal model for building forest NPP-age curves in China, and the model with the highest R^2 and smallest RMSE would be regarded as optimal.

3.3 Determination of ten forest NPP-age curves

Fig. 2 shows the statistics of forest field survey samples according to the three age groups in China. The age group of 0−50 years had the most samples in all forest cover types and regions. The regions NE and N mainly contained DBF (highest number), ENF, DNF, and MF sites. The region NW was dominated by the samples of DBF (highest number) and ENF. The region SW has the most samples of ENF and identical samples of EBF, DBF, and MF. Region S mainly had the samples of ENF (highest number), EBF, and DBF. The samples of EBF and ENF were dominant in region E. The age group of 51−100 years had fewer samples than the group of 0−50 years. EBF samples were mainly located in Region E and Region SW. The samples of ENF were identical for all six regions. The samples of DNF, DBF, and MF were dominant in the north (NE/N/NW) regions, and a few samples of DBF and MF were located in the south (SW/S/E) regions. The age group of >100 years had the lowest number of samples. The sample of ENF was dominant in the regions of NW and S. The sample of EBF was dominant in the regions E and S, and the sample of DNF was dominant in regions NW.

In consideration of the survey sample and stand age distribution patterns, ten forest NPP-age curves were derived across the entire China. The samples of EBF were sufficient to separate three forest NPP-age curves for the north (NE/N/NW) regions, the SW region, and the S/E regions. The samples of ENF, BDF, and MF were sufficient to build two separate forest NPP-age curves for the north (NE/N/NW) and south (SW/S/E) regions. The samples of DNF were rare and mainly located in the north (NE/N/NW) regions, and there was only one forest growth curve for DNF in the entire China.

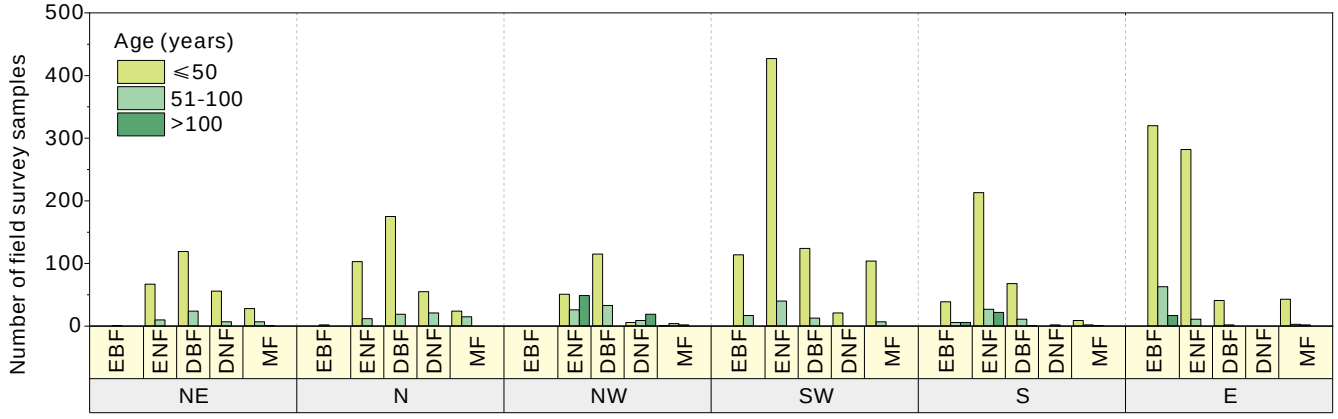

Figure 2. The statistics of forest field survey samples according to age groups, regions, and forest cover types in China. The first horizontal coordinate (yellow) indicates the region; the second horizontal coordinate (blue) indicates the forest cover type; the bar indicates the number of samples; and the bar colour indicates the age group (purple is for 0 to 50 years, green is for 51 to 100 years, and orange is for >100 years). E: Northeast China; N: North China; NW: Northwest China; E: East China; S: South China; SW: Southwest China; EBF: Evergreen Broad-

https://doi.org/10.5194/bg-2023-137
Preprint. Discussion started: 28 August 2023

leaved Forests; ENF: Evergreen Needle-leaved Forests; DBF: Deciduous Broad-leaved Forests; DNF: Deciduous Needle-leaved Forests; MF: Mixed Forests.

3.4 Uncertainty analysis

The uncertainty of an NPP-age curve mainly comes from the calculation of forest field NPP, whose uncertainty was calculated from its four components (Yu et al., 2017) in Equation (1). It was represented as the sum of the variances of four independently calculated values based on forest age group:

$$\sigma_{NPP}^2 = \sigma_{\triangle B_c}^2 + \sigma_M^2 + \sigma_{L_l}^2 + \sigma_{L_{fr}}^2, \quad (10)$$

where σ_{NPP}^2 is the uncertainty of the NPP-age curve, $\sigma_{\triangle B_c}^2$ is the uncertainty in the biomass measurements, σ_{M}^2 is the uncertainty in the mortality estimation, $\sigma_{L_l}^2$ and $\sigma_{L_{fr}}^2$ are the uncertainties in the estimates of the turnovers of leaves and fine roots, respectively. As L_l and L_{fr} were correlated, their errors were estimated as follows:

$$\sigma_{L_l+L_{fr}}^2 = \sigma_{L_l}^2 + \sigma_{L_{fr}}^2 + 2cov_{L_l,L_{fr}}, \quad (11)$$

where $\sigma_{L_l}^2$ is the standard deviation of the leaf renewal rate, $\sigma_{L_{fr}}^2$ is the standard deviation of the fine roots renewal rate, and $cov_{L_l,L_{fr}}$ is the covariance between L_l and L_{fr}, which was simplified as $cov_{L_l,L_{fr}} \approx cov_{L_l,R_{fr,l}\cdot L_l} = R_{fr,l} \times cov_{L_l,L_l} = R_{fr,l} \times \sigma_{L_l}^2$ (He et al., 2012).

4 Results

Five models were compared to determine the best model for simulating forest NPP-age curves for different regions and forest cover types in China (Fig. 3). The three components used for the calculation of forest field NPP are shown in Fig. 4, where the annual increment of total living biomass, turnovers of foliage, and turnovers of fine roots in the soil were symbolized by hollow squares, triangles, and diamonds accompanied by their standard deviations, respectively. The annual increment of total living biomass constitutes the predominant share of NPP, markedly surpassing the sum of other components in NPP. Despite their relatively minor proportions, the turnover rates of foliage and the fine roots in the soil are essential components of NPP (He et al., 2012). Across various forest types, the annual increment of total living biomass rises in early forest development, peaks mid-term, and later declines, consistent with the trajectory of NPP with age.

Each NPP-age curve was fitted by the five functions based on the average NPP calculated from the field survey samples with the same forest cover types and regions, and their performances were quantitatively described using RMSE and R^2 (Fig. 5). The highest R^2 (labelled in green colour) and the lowest RMSE (labelled in red colour) indicate the best performance of one of the five models. The SEM function and Γ function performed prominently in all ten curves, perfectly capturing the NPP variations with forest age. The SEM function had the highest R^2 and lowest RMSE for three curves of EBF (NE/N/NW), EBF (S/E), ENF (CHN), and had the lowest RMSE but comparable R^2 for five curves including ENF (NE/N/NW), ENF (SW/S/E),

https://doi.org/10.5194/bg-2023-137
Preprint. Discussion started: 28 August 2023

DBF (NE/N/NW), MF (NE/N/NW), and MF (SW/S/E). The Γ function had the highest R^2 and lowest RMSE for two curves of EBF (SW) and DBF (SW/S/E). The NPP-age variations were not well captured by the SDP function, L function, and M function: the declining trend of forest NPP in old ages was not captured by the L and M functions, and five constructed curves by the SDP function exhibited unreasonable declines in NPP for older forest ages (with NPP sharply decreasing to 0 before reaching 200 years). Even though the SDP function achieved a relatively high R^2 (<0.05 lower than the highest R^2) in building two curves of EBF (SW) and DBF (SW/S/E), it had 13%−88% larger RMSE than the lowest RMSE. The M function also reached a relatively high R^2 (<0.05 lower than the highest R^2) in building four curves of EBF (S/E), ENF (NE/N/NW), DBF (NE/N/NW), and MF (NE/N/NW), but it had 29%−124% larger RMSE than the lowest RMSE.

To further evaluate the performances of the SEM function and the Γ function, we extended the forest age to 300 years and normalized the built NPP-age curves by dividing each curve with its maximum NPP value (Fig. 6). The solid lines indicate the age period with field data (the rectangle in each line indicates the largest age in the field data), and the dashed lines indicate the predicted values at ages beyond the field data. The most significant differences between the normalized NPP-age curves simulated using these two functions appear in the extended old ages. The curves built from the SEM function exhibit stable forest NPP during old ages, while those from the Γ function display a distinct and continuous decrease in NPP as the forests become very old. For the two curves of EBF(SW) and DBF(SW/S/E) where the Γ function had the highest R^2 and lowest RMSE, the forest NPP decreased to almost zero when the stand age reached 300 years. The forest NPP in the curves of ENF(SW/S/E), MF(SW/S/E), DBF(NE/N/NW), and DNF(CHN) built by the Γ function also decreased more than 50 % in old ages. These forest growth patterns are unreasonable, as they suggest that forests would stop growth completely at old ages and act as carbon sources. However, studies have demonstrated that old forests still act as carbon sinks, despite the controversial magnitude of the forest carbon sink ranging from 1.0 to 3.2 Mg C ha^{-1} yr^{-1} (Gundersen et al., 2021; Luyssaert et al., 2008). Ecologically, we would expect old forests to maintain stable conditions through self-renewal processes, such as the generation of new trees after the mortality of old trees (Harmon et al., 1990). The SEM function that produces stable NPP at old ages is therefore more reasonable in capturing the forest NPP-age variations during old ages. These results suggested that the SEM function was determined as the best forest NPP-age model (the model coefficients of the built ten forest NPP-age curves in China are provided in Table 2).

https://doi.org/10.5194/bg-2023-137
Preprint. Discussion started: 28 August 2023

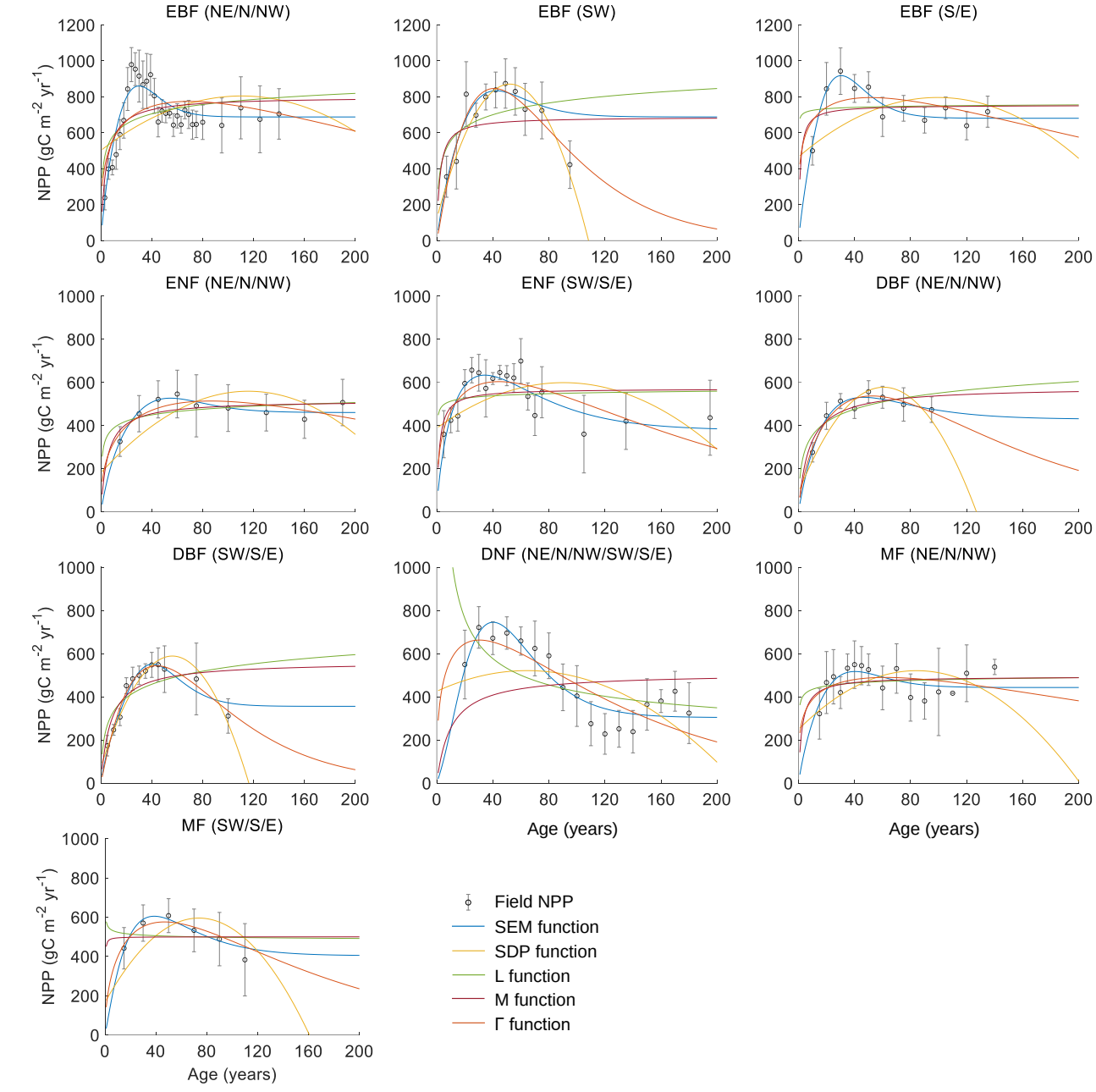

Figure 3. Comparing five models in building the forest NPP-age curves for different forest cover types and regions in China. In each panel, regions are shown in the upper right. The black hollow dots with error bars represent the average NPP and its one standard deviation. The five colourful lines indicate the curve-fitting from the five functions. E: Northeast China; N: North China; NW: Northwest China; E: East China; S: South China; SW: Southwest China; EBF: Evergreen Broad-leaved Forests; ENF: Evergreen Needle-leaved Forests; DBF: Deciduous Broad-leaved Forests; DNF: Deciduous Needle-leaved Forests; MF: Mixed Forests.

https://doi.org/10.5194/bg-2023-137
Preprint. Discussion started: 28 August 2023

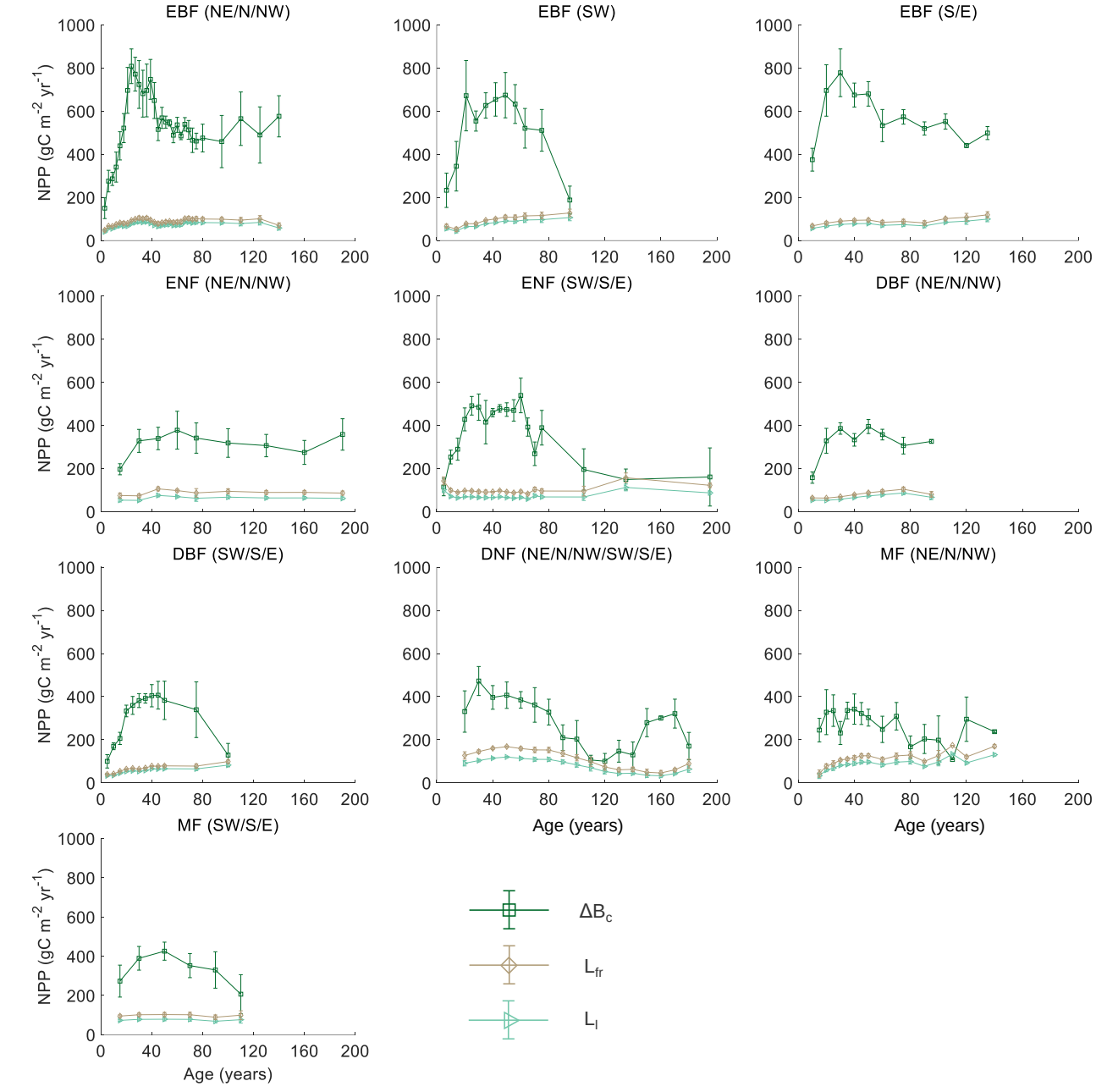

230 **Figure 4.** Distribution of the three components of NPP for different forest cover types and regions in China. Hollow points with error bars represent the components of NPP along with one standard deviation. $\triangle \boldsymbol{B_c}$ is the annual increment of total living biomass including stems, branches, and coarse roots; $\boldsymbol{L_l}$ is the turnover of leaves per year; and $\boldsymbol{L_{fr}}$ is the turnover of fine roots per year in the soil. E: Northeast China; N: North China; NW: Northwest China; E: East China; S: South China; SW: Southwest China; EBF: Evergreen Broad-leaved Forests; ENF: Evergreen Needle-leaved Forests; DBF: Deciduous Broad-leaved Forests; DNF: Deciduous Needle-leaved Forests; MF: Mixed Forests.

https://doi.org/10.5194/bg-2023-137
Preprint. Discussion started: 28 August 2023

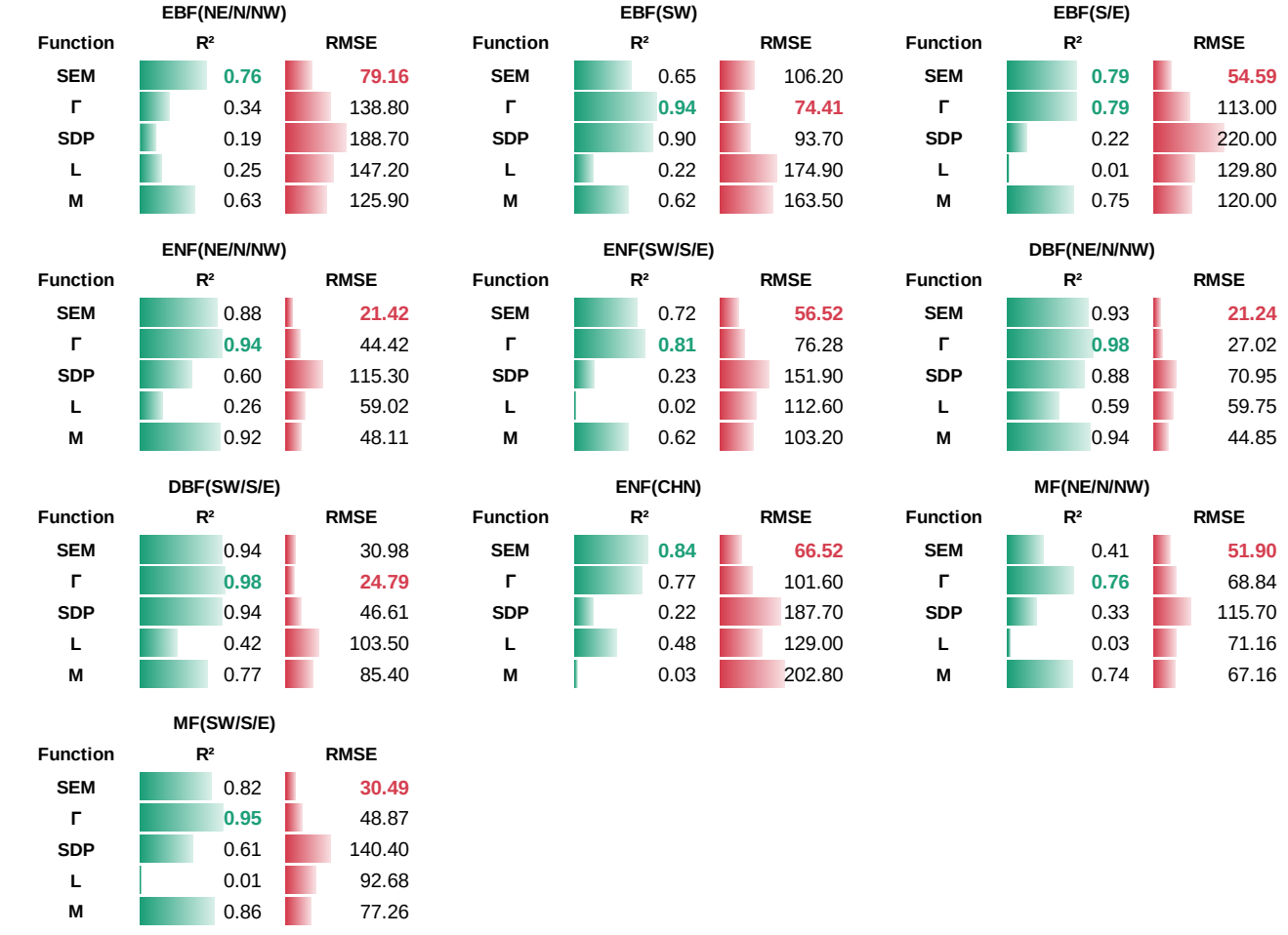

Figure 5. Quantitative descriptions of the five models in building the forest NPP-age curves for different forest cover types and regions in China. The highest R^2 is labelled with green colour, and the lowest RMSE is labelled with red colour. E: Northeast China; N: North China; NW: Northwest China; E: East China; S: South China; SW: Southwest China; EBF: Evergreen Broad-leaved Forests; ENF: Evergreen Needle-leaved Forests; DBF: Deciduous Broad-leaved Forests; DNF: Deciduous Needle-leaved Forests; MF: Mixed Forests.

https://doi.org/10.5194/bg-2023-137
Preprint. Discussion started: 28 August 2023

Biogeosciences Discussions Open Access EGU

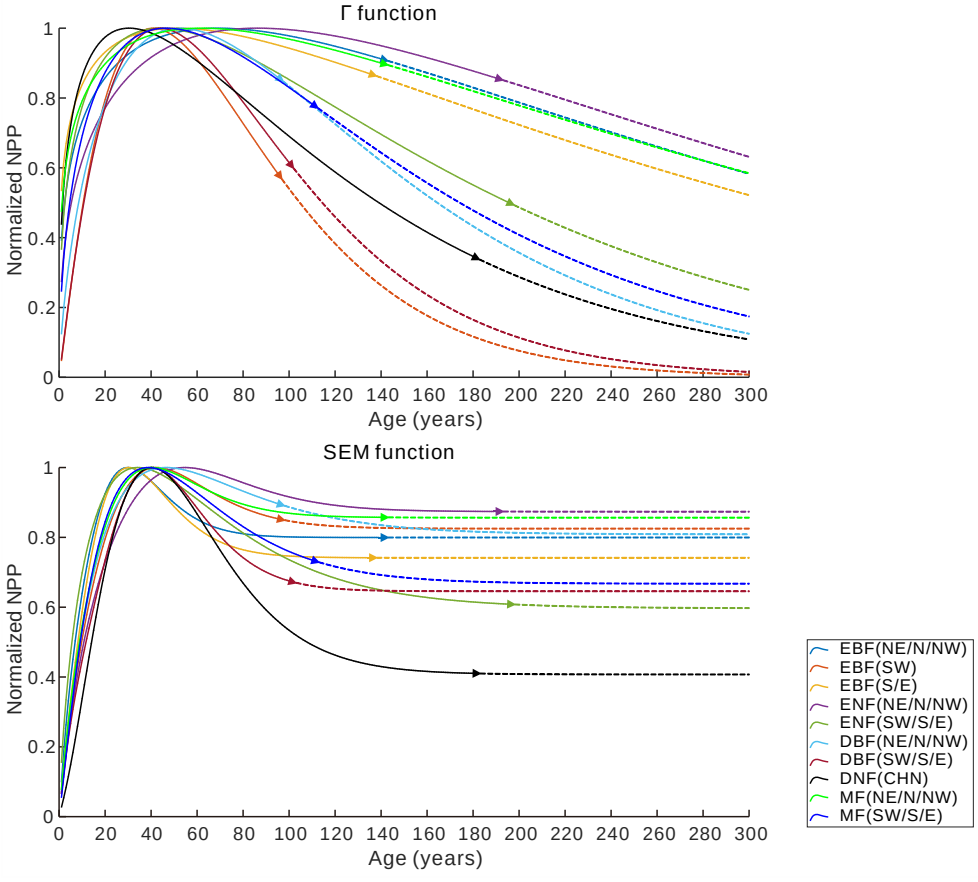

Figure 6. The normalized NPP-age curves built from the SEM function and the Γ function with the forest age extended to 300 years. The solid lines are for the age period with field data (the triangle in each line indicates the largest age with the field data), and the dashed lines are for the age period without field data. E: Northeast China; N: North China; NW: Northwest China; E: East China; S: South China; SW: Southwest China; EBF: Evergreen Broad-leaved Forests; ENF: Evergreen Needle-leaved Forests; DBF: Deciduous Broad-leaved Forests; DNF: Deciduous Needle-leaved Forests; MF: Mixed Forests.

Table 2. The coefficients of the built forest NPP-age curves by the SEM function in China. **a**-**d**: the model coefficients; E: Northeast China; N: North China; NW: Northwest China; E: East China; S: South China; SW: Southwest China; EBF: Evergreen Broad-leaved Forests; ENF: Evergreen Needle-leaved Forests; DBF: Deciduous Broad-leaved Forests; DNF: Deciduous Needle-leaved Forests; MF: Mixed Forests.

Forest Type	*a*	b	*c*	d
EBF(NE/N/NW)	687.549	0.094	7.613	3.643
ENF(SW)	687.726	0.126	11.467	3.310
EBF(S/E)	680.323	0.280	9.108	3.032
ENF(NE/N/NW)	460.192	0.045	13.007	3.809
ENF(SW/S/E)	378.106	2.828	31.679	0.721
DBF(NE/N/NW)	429.184	1.353	26.832	0.995
DBF(SW/S/E)	355.632	0.097	9.508	4.153
DNF(CHN)	303.573	2.029	15.739	2.425
MF(NE/N/NW)	442.899	0.105	10.750	3.290
MF(SW/S/E)	403.397	1.926	22.778	1.245

https://doi.org/10.5194/bg-2023-137
Preprint. Discussion started: 28 August 2023

5 Discussion

In this study, we derived ten forest NPP-age curves for six regions and five forest cover types in China based on 3121 forest field samples (Fang et al., 2018) and tested five mathematical models including the SEM function, SDP function, L function, M function, and Γ function for simulating the curves. The SEM function and Γ function performed prominently in fitting all ten curves, nearly perfectly capturing NPP variations with forest age; while for the SDP function, L function, and M function, the NPP-age variations were not well captured. The declining trend of forest NPP in old ages was not captured by the L function and M function, while the SDP function exhibited a sharp decline of NPP to 0 before reaching 200 years in five forest NPP-age curves. These results were consistent with the study that compared NPP-age relationships in boreal and temporal forests constructed using the SDP function, L function, M function, and Γ function (Tang et al., 2014). Further analysis using the normalized NPP-age curves with forest age extended to 300 years suggested that the SEM function was generally more applicable than the Γ function for tracking NPP variation with forest age. In particular, the SEM function produces stable NPP at very old ages, while the Γ function unreasonably forces NPP to be zero at old ages.

5.1 The mechanism of NPP-age variations

The forest NPP exhibits a rapid increase during young ages, reaching a peak in a middle age, and subsequently declining in old age (Chen et al., 2003; Yu et al., 2017; He et al., 2012). Previous understanding attributed the decline in NPP in aging forests primarily to the reduction in gross primary productivity (GPP) as the forest ages, while autotrophic respiration (Ra) increases with age (Tatuo KIRA and SHIDEI, 1967; Odum, 1969). However, recent studies have challenged this classical view, revealing that the age-driven decline in NPP is primarily driven by the decrease in both GPP and Ra as forests age, with GPP declining at a faster rate than Ra (Drake et al., 2011; Ryan et al., 1997, 2004; Ryan and Waring, 1992; Tang et al., 2014). This decline in forest NPP during old ages can be attributed to nutrient limitation and ecosystem succession (Camenzind et al., 2018; Fisher et al., 2012; Gao et al., 2018; Gough et al., 2008). However, old forests can maintain stable growth conditions through self-renewal and continue to accumulate carbon with a magnitude of carbon sinks ranging from 1.0 to 3.2 Mg C ha^{-1} yr^{-1} (Gundersen et al., 2021; Luyssaert et al., 2008).

5.2 Comparison to the forest NPP-age curves built previously in China

The forest NPP-age curve could be depicted by a key characteristic: the age at which forest NPP peaks (shortened as peak NPP age). The ten built forest NPP-age curves by the SEM function in this study were compared to the forest NPP-age curves built previously in China using this characteristic (Table 3). Climate factors have a significant influence on the peak NPP age (Zhang et al., 2017). The NPP-age curves of forests in southern regions, characterized by higher temperatures, generally exhibit an earlier age of peak NPP compared to forests in the northern regions with lower temperatures.

EBF achieves its highest NPP at 30 years in the regions of NE/N/NW/S/E, while this peak occurs at 42 years in region SW, similar to the previously reported average peak age of 40 years for EBF in China (Wang et al., 2011). The peak NPP for ENF

https://doi.org/10.5194/bg-2023-137
Preprint. Discussion started: 28 August 2023

is achieved at 55 years in the northern regions, while it occurs at 34 years in the southern regions, aligned with previous reports where the peak age in the northern regions is 21 years later compared to the southern regions (Xu et al., 2010). But in the southern regions, our peak NPP age of 34 years was significantly different from the 13 years reported by Wang et al. (2011). However, their fitting points showed a significant bimodal distribution around 13 and 53 years. Considering this bimodal distribution, the average peak NPP age could be 33 years, more closely to our findings.

DBF, predominantly located in the northern regions, peaks in NPP at the age of 47, slightly later than the southern regions where the peak is observed at 41 years. These two values were much smaller than the 122 years reported by Wang et al. (2011), where the NPP-age curve for DBF was built by the SDP function instead of the SEM function. This large difference for DBF was also noticed by He et al. (2012), and our results were consistent with the peak NPP age of 27 ± 16.5 for BDFs in America (He et al., 2012).

DNF, 60.2% located in the northern regions, reaches peak NPP at the age of 40 years, congruent with the peak growth age derived from the same region by other researchers using the Logistic stand growth model with National Forest Inventory (NFI) data (Xu et al., 2010). Our peak age differed by 14 years from the 54 years reported by Wang et al. (2011). However, their fitting points demonstrated that the peak NPP spanned ages from 20 to 70 years (Wang et al., 2011), with an average of 45 years, which aligns more closely with our peak NPP age.

MF reached the peak NPP at the age of 40 in the northern regions and 39 years in the southern regions, presenting a deviation of less than 8 years compared to Wang et al. (2011) and a consistent peak NPP reported in Heilongjiang province by Yu et al. (2017). The peak NPP age of our national NPP-age curve shows substantial differences from the peak NPP ages identified by Yu et al. (2017) and Zheng et al. (2019) in their respective studies on the Heilongjiang and Zhejiang provinces. This could be attributed to significant variations in forest growth patterns nationwide compared to these specific provinces, arising from various factors including but not limited to forest species, climatic conditions, and soil types (Dai et al., 2011; Zhao and Zhou, 2006; Ji et al., 2020; Xiaoyun et al., 2018).

Table 3. Comparison of the forest NPP-age curves built previously in China at the peak NPP age. E: Northeast China; N: North China; NW: Northwest China; E: East China; S: South China; SW: Southwest China; EBF: Evergreen Broad-leaved Forests; ENF: Evergreen Needle-leaved Forests; DBF: Deciduous Broad-leaved Forests; DNF: Deciduous Needle-leaved Forests; MF: Mixed Forests; ENF-S: ENF in the tropics and subtropics; MBF: Mixed Broad-leaved Forests; ENF-H: ENF in Heilongjiang province, including Pinus sylvestris and Pinus koraiensis; DBF-H: DBF in Heilongjiang province, including Quercus mongolica, Planted populus, Populus davidiana, Betula davuria, Tilia, and Betula platyphylla; DNF-H: Larix gmelinii in Heilongjiang province; MBF-H: Mixed Broad-leaved Forests in Heilongjiang province; MNF-H: Mixed Needle-leaved Forest in Heilongjiang province; MF-H: Mixed Forests in Heilongjiang province; NF-Z: Needle-leaved Forest in Zhejiang province; BF-Z: Broad-leaved Forest in Zhejiang province.

Study area	Forest type	China regions	Methods	Age at peak NPP (year)	Source
China	EBF	NE/N/NW	SEM	30	This study
		SW		42	
		S/E		30	
	ENF	NE/N/NW		55	
		SW/S/E		34	

https://doi.org/10.5194/bg-2023-137
Preprint. Discussion started: 28 August 2023

	DBF	NE/N/NW		47	
		SW/S/E		41	
	DNF	CHN		40	
	MF	NE/N/NW		40	
		SW/S/E		39	
China	EBF	CHN	SEM	40	Wang et al. (2011)
	ENF-S	SW/S/E	SEM	13	
	DBF	CHN	SDP	122	
	DNF	CHN	SEM	54	
	MBF	CHN	SEM	32	
Heilongjiang	ENF-H	---	SEM	19 ± 4.2	Yu et al. (2017)
	DBF-H			11 ± 5.1	
	DNF-H			20 ± 2.7	
	MBF-H			11 ± 2.0	
	MNF-H			39 ± 7.4	
	MF-H			16 ± 1.9	
Zhejiang	NF-Z	---	SEM	23	Zheng et al. (2019)
	BF-Z			15	

5.3 Limitations and future modifications

There were also some limitations in this study. First, considering the sample numbers, distributions, and age groups, only ten forest NPP-age curves were derived across the entire China. Except for DNF, the differences in forest NPP-age curves between the southern and northern regions of China (Dai et al., 2011) were considered for all forest cover types. For EBF, its samples were sufficient to separate two forest NPP-age curves in southern China: one is for region SW, and the other is for the regions of S/E. The constructed forest NPP-age curve may not be universally applicable to all areas within the region or specific forest types. For future modifications, it is advisable to incorporate additional samples and develop separate NPP-age curves tailored to smaller regions.

Second, in the calculation of the field NPP, we did not account for the mortality due to the lack of data and its small proportion of NPP (3.7% on average, calculated using the data in America (He et al., 2012)). The turnovers of leaves and fine roots, which were also two important components of the field NPP, were calculated based on the assumption that fine root production is linearly correlated with the production of leaves (Litton et al., 2007; He et al., 2012). This assumption was supported by the correlation between new fine root carbon and new leaf carbon indicated by the field measurements (Børja et al., 2008; Burkes et al., 2003; Claus and George, 2005; DesRochers and Lieffers, 2001). It should be noted that fine root production could also be affected by other factors such as soil texture, moisture, and climate (Zerihun and Montagu, 2004), which might be calculated from other carbon allocation methods in future modifications (White et al., 2000).

https://doi.org/10.5194/bg-2023-137
Preprint. Discussion started: 28 August 2023

Last, the site condition was not considered in building the forest NPP-age curves. It has been shown that the site condition can impact the forest NPP-age variations, and better site conditions can result in faster growth of NPP in young age, greater peak NPP, and steeper decline of NPP in old ages (Yu et al., 2017; Wang et al., 2018). However, the lack of site condition data impeded our ability to build separate forest NPP-age curves according to the site conditions. Regardless of these limitations, this study still provides valuable insights into forest NPP-age variations, and collecting more comprehensive data in the future can further enhance the construction of forest NPP-age curves.

6 Conclusions

In this study, we investigated the relationship between forest NPP and age in China by using 3121 forest field survey samples and remote sensing data. Ten forest NPP-age curves were derived for all China's forests based on the spatial distributions of forest cover type, biomass, and age of the field survey data. Five models, including the SEM function, SDP function, L function, M function, and Γ function, were compared to determine the optimal model for building the forest NPP-age curves in China. The comparison against the survey data showed that the SEM function and the Γ function performed much better than the other three models, and through extending forest ages to 300 years, we found that the SEM function was more reasonable than the Γ function in capturing stable NPP at old ages. The built forest NPP-age curves offer an independent and comprehensive source of information for forest growth estimation and can facilitate forest carbon modelling and future carbon projections in China and elsewhere.

Code availability

The codes for building forest NPP-age relationships are available by request from the corresponding authors.

Data availability

The coefficients of the built forest NPP-age relationships are available in Table 2.

Author contribution

Conceptualization, R.S. and J.M.C.; Methodology, P.L., R.S. and J.M.C.; Validation, P.L.; Formal analysis, P.L., M.X. and X.L.; Writing—original draft, P.L. and R.S.; Writing—review & editing, R.S., J.M.C. and M.X.; Funding acquisition, R.S. and M.X. Data curation, G.Y., N.H. and L.X..

https://doi.org/10.5194/bg-2023-137
Preprint. Discussion started: 28 August 2023

Competing interests

The authors declare that they have no conflict of interest.

Acknowledgments

This research was funded by the National Natural Science Foundation of China (42101367 and 42201360), the Natural Science Foundation of Fujian Province (2021J05041), the Fujian Forestry Science and Technology Key Project (2022FKJ03), and the Open Fund Project of the Academy of Carbon Neutrality of Fujian Normal University (TZH2022-02).

References

Alexandrov, G. A., Oikawa, T., and Esser, G.: Estimating terrestrial NPP: what the data say and how they may be interpreted?, Ecol. Modell., 117, 361–369, https://doi.org/10.1016/S0304-3800(99)00019-8, 1999.

Bond-Lamberty, B., Wang, C., and Gower, S. T.: Net primary production and net ecosystem production of a boreal black spruce wildfire chronosequence, Glob. Chang. Biol., 10, 473–487, https://doi.org/10.1111/j.1529-8817.2003.0742.x, 2004.

Burkes, E. C., Will, R. E., Barron-Gafford, G. A., Teskey, R. O., and Shiver, B.: Biomass partitioning and growth efficiency of intensively managed Pinus taeda and Pinus elliottii stands of different planting densities, For. Sci., 49, 224–234, https://doi.org/10.1093/forestscience/49.2.224, 2003.

Camenzind, T., Hättenschwiler, S., Treseder, K. K., Lehmann, A., and Rillig, M. C.: Nutrient limitation of soil microbial processes in tropical forests, Ecol. Monogr., 88, 4–21, https://doi.org/10.1002/ecm.1279, 2018.

Chapin, F. S., III, Woodwell, G. M., Randerson, J. T., Rastetter, E. B., Lovett, G. M., Baldocchi, D. D., Clark, D. A., Harmon, M. E., and Schimel, D. S.: Reconciling Carbon-Cycle Concepts, Terminology, and Methods, Ecosystems, 9, 1041–1050, https://doi.org/10.1007/s10021-005-0105-7, 2006.

Chen, J. M., Ju, W., Cihlar, J., Price, D., Liu, J., Chen, W., Pan, J., Black, A., and Barr, A.: Spatial distribution of carbon sources and sinks in Canada's forests, Tellus B Chem. Phys. Meteorol., 55, 622, https://doi.org/10.3402/tellusb.v55i2.16711, 2003.

Chen, J. M., Mo, G., Pisek, J., Liu, J., Deng, F., Ishizawa, M., and Chan, D.: Effects of foliage clumping on the estimation of global terrestrial gross primary productivity, Global Biogeochem. Cycles, 26, https://doi.org/10.1029/2010GB003996, 2012.

Chen, W., Chen, J. M., Price, D. T., and Cihlar, J.: Effects of stand age on net primary productivity of boreal black spruce forests in Ontario, Canada, Can. J. For. Res., 32, 833–842, https://doi.org/10.1139/x01-165, 2002.

Dai, L., Wang, Y., Su, D., Zhou, L., Yu, D., Lewis, B. J., and Qi, L.: Major forest types and the evolution of sustainable forestry in China, Environ. Manage., 48, 1066–1078, https://doi.org/10.1007/s00267-011-9706-4, 2011.

https://doi.org/10.5194/bg-2023-137
Preprint. Discussion started: 28 August 2023

380 Dalgleish, S. A., Van Etten, E. J. B., Stock, W. D., and Knuckey, C.: Fuel dynamics and vegetation recovery after fire in a semiarid Australian shrubland, Int. J. Wildl. Fire, 24, 613–623, https://doi.org/10.1071/WF14128, 2015.

DesRochers, A. and Lieffers, V. J.: Root biomass of regenerating aspen (Populus tremuloides) stands of different densities in Alberta, Can. J. For. Res., 31, 1012–1018, https://doi.org/10.1139/x01-037, 2001.

Do, H. T. T., Zimmer, H. C., Vanclay, J. K., Grant, J. C., Trinh, B. N., Nguyen, H. H., and Nichols, J. D.: Site form
385 classification - a practical tool for guiding site-specific tropical forest landscape restoration and management, Forestry, 95, 261–273, https://doi.org/10.1093/forestry/cpab046, 2022.

Drake, J. E., Davis, S. C., Raetz, L. M., and Delucia, E. H.: Mechanisms of age-related changes in forest production: The influence of physiological and successional changes, Glob. Chang. Biol., 17, 1522–1535, https://doi.org/10.1111/j.1365-2486.2010.02342.x, 2011.

390 Eggleston, S., Buendia, L., Miwa, K., Ngara, T., and Tanabe, K.: 2006 IPCC Guidelines for National Greenhouse Gas Inventories. V.4. Agriculture, Forestry and Other Land Use, 2006.

Fang, J., Chen, A., Peng, C., Zhao, S., and Ci, L.: Changes in forest biomass carbon storage in China between 1949 and 1998, Science (80-.)., 292, 2320–2322, https://doi.org/10.1126/science.1058629, 2001.

Fang, J., Yu, G., Liu, L., Hu, S., and Stuart Chapin, F.: Climate change, human impacts, and carbon sequestration in China,
395 Proc. Natl. Acad. Sci. U. S. A., 115, 4015–4020, https://doi.org/10.1073/pnas.1700304115, 2018.

Fang Jingyun , Ke Jinhu , Tang Zhiyao, C. E. A.: Implications and estimations of four terrestrial productivity parameters, Acta Phytoecol. Sin., 25, 414–419, 2001.

Fisher, J. B., Badgley, G., and Blyth, E.: Global nutrient limitation in terrestrial vegetation, Global Biogeochemical Cycles, John Wiley & Sons, Ltd, https://doi.org/10.1029/2011GB004252, 2012.

400 Friedlingstein: Global Carbon Budget 2020 : Global Carbon Project, Earth System Science Data., 12, 3269–3340, https://doi.org/10.3929/ethz-b-000458765, 2020.

Gao, B., Taylor, A. R., Searle, E. B., Kumar, P., Ma, Z., Hume, A. M., and Chen, H. Y. H.: Carbon Storage Declines in Old Boreal Forests Irrespective of Succession Pathway, Ecosystems, 21, 1168–1182, https://doi.org/10.1007/s10021-017-0210-4, 2018.

405 Gough, C. M., Vogel, C. S., Schmid, H. P., and Curtis, P. S.: Controls on annual forest carbon storage: Lessons from the past and predictions for the future, Bioscience, 58, 609–622, https://doi.org/10.1641/B580708, 2008.

Gower, ST, Vogel, JG, Norman, JM, Kucharik, CJ, Steele, and SJ: Carbon distribution and aboveground net primary production in aspen, jack pine, and black spruce stands in Saskatchewan and Manitoba, Canada, J. Geophys. Res. Atmos., 102, 29029–29041, https://doi.org/10.1029/97JD02317, 1997.

410 Gundersen, P., Thybring, E. E., Nord-Larsen, T., Vesterdal, L., Nadelhoffer, K. J., and Johannsen, V. K.: Old-growth forest carbon sinks overestimated, Nature, 591, E21–E23, https://doi.org/10.1038/s41586-021-03266-z, 2021.

Guo, L., An, N., and Wang, K.: Journal of geophysical research, Nature, 175, 238, https://doi.org/10.1038/175238c0, 1955.

Harmon, M. E., Ferrell, W. K., and Franklin, J. F.: Effects on carbon storage of conversion of old-growth forests to young forests, Science (80-.)., 247, 699–702, https://doi.org/10.1126/science.247.4943.699, 1990.

Hasenauer, S., Mag, and Sulzer, W.: the significance of remote sensing in the good practice guidance for land use, land-use change and forestry as specified by the kyoto protocol diploma thesis, 2004.

He, L., Chen, J. M., Pan, Y., Birdsey, R., and Kattge, J.: Relationships between net primary productivity and forest stand age in U.S. forests, Global Biogeochem. Cycles, 26, 1–19, https://doi.org/10.1029/2010GB003942, 2012.

Hicke, J. A., Jenkins, J. C., and Ducey, O. M.: Spatial Patterns of Forest Characteristics in the Western United States Derived from Inventories, Ecol. Appl., 17, 2387–2402, https://doi.org/https://doi.org/10.1890/06-1951.1, 2007.

Ji, Y., Zhou, G., Luo, T., Dan, Y., Zhou, L., and Lv, X.: Variation of net primary productivity and its drivers in China's forests during 2000–2018, For. Ecosyst., 7, https://doi.org/10.1186/s40663-020-00229-0, 2020.

Ju, W., Chen, J. M., Black, T. A., Barr, A. G., Liu, J., and Chen, B.: Modelling multi-year coupled carbon and water fluxes in a boreal aspen forest, Agric. For. Meteorol., 140, 136–151, https://doi.org/10.1016/j.agrformet.2006.08.008, 2006.

Litton, C. M., Raich, J. W., and Ryan, M. G.: Carbon allocation in forest ecosystems, Glob. Chang. Biol., 13, 2089–2109, https://doi.org/10.1111/j.1365-2486.2007.01420.x, 2007.

Liu, H., Gong, P., Wang, J., Wang, X., Ning, G., and Xu, B.: Production of global daily seamless data cubes and quantification of global land cover change from 1985 to 2020 - iMap World 1.0, Remote Sens. Environ., 258, 112364, https://doi.org/10.1016/j.rse.2021.112364, 2021.

Liu, J., Chen, J. M., Cihlar, J., and Chen, W.: Net primary productivity distribution in the BOREAS region from a process model using satellite and surface data, J. Geophys. Res. Atmos., 104, 27735–27754, https://doi.org/10.1029/1999JD900768, 1999.

Liu, J., Chen, J. M., Cihlar, J., and Chen, W.: Net primary productivity mapped for Canada at 1-km resolution, Glob. Ecol. Biogeogr., 11, 115–129, https://doi.org/10.1046/j.1466-822X.2002.00278.x, 2002.

Liu, Y., Liu, R., and Chen, J. M.: Retrospective retrieval of long-term consistent global leaf area index (1981-2011) from combined AVHRR and MODIS data, J. Geophys. Res. Biogeosciences, 117, 1–14, https://doi.org/10.1029/2012JG002084, 2012.

Liu Yingchun, Yu Guirui, Wang Qiufeng, and Zhang Yangjian: Huge Carbon Sequestration Potential in Global Forests, J. Resour. Ecol., 3, 193–201, https://doi.org/10.5814/j.issn.1674-764x.2012.03.001, 2012.

Luyssaert, S., Schulze, E. D., Börner, A., Knohl, A., Hessenmöller, D., Law, B. E., Ciais, P., and Grace, J.: Old-growth forests as global carbon sinks, Nature, 455, 213–215, https://doi.org/10.1038/nature07276, 2008.

Odum, E. P.: The strategy of ecosystem development, Science (80-.)., 164, 262–270, https://doi.org/10.1126/science.164.3877.262, 1969.

Pan, Y., Birdsey, R. A., Fang, J., Houghton, R., Kauppi, P. E., Kurz, W. A., Phillips, O. L., Shvidenko, A., Lewis, S. L., Canadell, J. G., Ciais, P., Jackson, R. B., Pacala, S. W., McGuire, A. D., Piao, S., Rautiainen, A., Sitch, S., and Hayes,

D.: A Large and Persistent Carbon Sink in the World's Forests, Science (80-.)., 333, 988–993, https://doi.org/10.1126/science.1201609, 2011.

Peper, P. J., McPherson, G. E., and Mori, S. M.: Predictive equations for dimensions and leaf area of coastal Southern California street trees, Journal of Arboriculture., 27, 169-180, https://doi.org/10.48044/jauf.2001.019, 2001.

Ryan, M. G. and Waring, R. H.: Maintenance Respiration and Stand Development in a Subalpine Lodgepole Pine Forest, Ecology, 73, 2100–2108, https://doi.org/https://doi.org/10.2307/1941458, 1992.

Ryan, M. G., Binkley, D., and Fownes, J. H.: Age-Related Decline in Forest Productivity: Pattern and Process, vol. 27, edited by: Begon, M. and Fitter, A. H. B. T.-A. in E. R., Academic Press, 213–262, https://doi.org/10.1016/S0065-2504(08)60009-4, 1997.

Ryan, M. G., Binkley, D., Fownes, J. H., Giardina, C. P., and Senock, R. S.: An experimental test of the causes of forest growth decline with stand age, Ecol. Monogr., 74, 393–414, https://doi.org/10.1890/03-4037, 2004.

Semenzato, P., Cattaneo, D., and Dainese, M.: Growth prediction for five tree species in an Italian urban forest, Urban For. Urban Green., 10, 169–176, https://doi.org/10.1016/j.ufug.2011.05.001, 2011.

Sönke Zaehle, Stephen Sitch, I. Colin Prentice, Jari Liski, Wolfgang Cramer, Markus Erhard, Thomas Hickler, B. S.: The importance of age-related decline in forest NPP for modeling regional carbon balances, Ecol. Appl., 16, 1555–1574, https://doi.org/10.1890/1051-0761(2006)016[1555:TIOADI]2.0.CO;2, 2006.

Tang, J., Luyssaert, S., Richardson, A. D., Kutsch, W., and Janssens, I. A.: Steeper declines in forest photosynthesis than respiration explain age-driven decreases in forest growth, Proc. Natl. Acad. Sci. U. S. A., 111, 8856–8860, https://doi.org/10.1073/pnas.1320761111, 2014.

Tang, X., Zhao, X., Bai, Y., Tang, Z., Wang, W., Zhao, Y., Wan, H., Xie, Z., Shi, X., Wu, B., Wang, G., Yan, J., Ma, K., Du, S., Li, S., Han, S., Ma, Y., Hu, H., He, N., Yang, Y., Han, W., He, H., Yu, G., Fang, J., and Zhou, G.: Carbon pools in China's terrestrial ecosystems: New estimates based on an intensive field survey, Proc. Natl. Acad. Sci. U. S. A., 115, 4021–4026, https://doi.org/10.1073/pnas.1700291115, 2018.

Tatuo KIRA and SHIDEI, T.: Primary production and turnover of organic matter in different forest ecosystems of the western Pacific, Japanese J. Ecol., 17, 70–87, https://doi.org/10.18960/seitai.17.2_70, 1967.

Van Tuyl, S., Law, B. E., Turner, D. P., and Gitelman, A. I.: Variability in net primary production and carbon storage in biomass across Oregon forests - an assessment integrating data from forest inventories, intensive sites, and remote sensing, For. Ecol. Manage., 209, 273–291, https://doi.org/10.1016/j.foreco.2005.02.002, 2005.

Wang, B., Li, M., Fan, W., Yu, Y., and Chen, J. M.: Relationship between net primary productivity and forest stand age under different site conditions and its implications for regional carbon cycle study, Forests, 9, 5, https://doi.org/10.3390/f9010005, 2018.

Wang, S., Chen, J. M., Ju, W. M., Feng, X., Chen, M., Chen, P., and Yu, G.: Carbon sinks and sources in China's forests during 1901-2001, J. Environ. Manage., 85, 524–537, https://doi.org/10.1016/j.jenvman.2006.09.019, 2007.

Wang, S., Zhou, L., Chen, J., Ju, W., Feng, X., and Wu, W.: Relationships between net primary productivity and stand age for several forest types and their influence on China's carbon balance, J. Environ. Manage., 92, 1651–1662, https://doi.org/10.1016/j.jenvman.2011.01.024, 2011.

White, M. A., Thornton, P. E., Running, S. W., and Nemani, R. R.: Parameterization and Sensitivity Analysis of the BIOME–BGC Terrestrial Ecosystem Model: Net Primary Production Controls, Earth Interact., 4, 1–85, https://doi.org/10.1175/1087-3562(2000)004<0003:pasaot>2.0.co;2, 2000.

Xia, J., Yuan, W., Lienert, S., Joos, F., Ciais, P., Viovy, N., Wang, Y. ping, Wang, X., Zhang, H., Chen, Y., and Tian, X.: Global Patterns in Net Primary Production Allocation Regulated by Environmental Conditions and Forest Stand Age: A Model-Data Comparison, J. Geophys. Res. Biogeosciences, 124, 2039–2059, https://doi.org/10.1029/2018JG004777, 2019.

Xiaoyun, Z., Minghang, G., and Tibin, Z.: Joint control of net primary productivity by climate and soil nitrogen in the forests of Eastern China, Forests, 9, 322, https://doi.org/10.3390/f9060322, 2018.

Xu, B., Guo, Z. Di, Piao, S. L., and Fang, J. Y.: Biomass carbon stocks in China's forests between 2000 and 2050: A prediction based on forest biomass-age relationships, Sci. China Life Sci., 53, 776–783, https://doi.org/10.1007/s11427-010-4030-4, 2010.

Yu, Y., Chen, J. M., Yang, X., Fan, W., Li, M., and He, L.: Influence of site index on the relationship between forest net primary productivity and stand age, PLoS One, 12, 1–20, https://doi.org/10.1371/JOURNAL.PONE.0177084, 2017.

Zerihun, A. and Montagu, K. D.: Belowground to aboveground biomass ratio and vertical root distribution responses of mature Pinus radiata stands to phosphorus fertilization at planting, Can. J. For. Res., 34, 1883–1894, https://doi.org/10.1139/X04-069, 2004.

Zha, T. S., Barr, A. G., Bernier, P. Y., Lavigne, M. B., Trofymow, J. A., Amiro, B. D., Arain, M. A., Bhatti, J. S., Black, T. A., and Margolis, H. A.: Gross and aboveground net primary production at Canadian forest carbon flux sites, Agric. For. Meteorol., 174–175, 54–64, https://doi.org/10.1016/j.agrformet.2013.02.004, 2013.

Zhang, Y., Yao, Y., Wang, X., Liu, Y., and Piao, S.: Mapping spatial distribution of forest age in China, Earth Sp. Sci., 4, 108–116, https://doi.org/10.1002/2016EA000177, 2017.

Zhao, M. and Zhou, G. S.: Estimation of biomass and net primary productivity of major planted forests in China based on forest inventory data, For. Ecol. Manage., 207, 295–313, https://doi.org/10.1016/j.foreco.2004.10.049, 2005.

Zhao, M. and Zhou, G. S.: Estimating net primary productivity of Chinese pine forests based on forest inventory data, Forestry, 79, 231–239, https://doi.org/10.1093/forestry/cpl002, 2006.

Zheng, J., Mao, F., Du, H., Li, X., Zhou, G., Dong, L., Zhang, M., Han, N., Liu, T., and Xing, L.: Spatiotemporal simulation of net ecosystem productivity and its response to climate change in subtropical forests, Forests, 10, 708, https://doi.org/10.3390/f10080708, 2019.